

## Femtosecond Laser-driven Soft X-Ray Sources for Time-resolved Spectroscopy

*Katsuya Oguri<sup>†</sup>, Yasuaki Okano, Tadashi Nishikawa, and Hidetoshi Nakano*

### Abstract

We are studying time-resolved x-ray absorption fine structure (XAFS) techniques using a femtosecond-laser-produced plasma x-ray source to measure ultrafast dynamics by x-ray absorption spectroscopy. In this paper, we describe the enhancement of x-ray emission intensity achieved by using nanostructured targets to improve the x-ray fluence. We also report a demonstration of the time-resolved XAFS technique applied to the laser-induced dynamics of Si foil. Our results clearly show the potential of the time-resolved XAFS technique for capturing ultrafast changes in the electronic state and atomic structure of materials.

### 1. Introduction

X-rays were discovered and named by Röntgen in 1895. They were a new type of radiation and their discovery had a huge effect on scientists throughout the world. Since then, various x-ray techniques have been developed for investigating the structural and electronic properties of matter using the unique feature of x-rays, namely that they mainly interact with localized core electrons. X-ray techniques using two main x-ray sources—conventional x-ray tubes and synchrotron sources—have helped drive rapid advances in our understanding of the static or time-averaged properties of matter. Such x-ray research has become well established as one of the most important fields in physics, chemistry, and biology, and it is now called x-ray science.

Recently, new x-ray sources that can generate x-ray pulses with a duration of a few picoseconds ( $10^{-12}$  s) down to the femtosecond ( $10^{-15}$  s) level have been developed as a result of the great technological progress made on high-power and ultrashort-pulse lasers. The emergence of these laser-based ultrashort-pulse x-ray sources (hereafter shortened to ultrashort

x-ray sources) has opened up new horizons for x-ray science, i.e., the study of the dynamic behavior of matter on a picosecond or femtosecond timescale by means of time-resolved measurements using ultrashort x-ray pulses. Since this time scale corresponds to one vibrational period, typically of the order of  $10^{-13}$  s (100 fs), these time-resolved x-ray techniques will provide us with a deep and clear insight into the ultrafast dynamics of matter on the atomic size and timescale. Currently, the study of ultrafast dynamic processes on this timescale, known as ultrafast science, is generally carried out with ultrafast optical techniques based on sophisticated femtosecond laser technology. This research field now covers matter ranging from molecules to solids [1], [2], and its scientific importance was recognized with the award of the 1999 Nobel Prize for Chemistry to A. H. Zewail. However, optical photons probe only valence electronic states, which usually include the superposition of multiple atoms, so access to information about the electronic states of specific atoms or their atomic arrangement is limited in methods that use optical photons. If we use x-ray photons instead of optical photons, we can expect to observe processes that occur during the making and breaking of chemical bonds and during atomic rearrangements in photoinduced chemical reactions or phase transformations. This provides a “movie” of a chemical reaction,

<sup>†</sup> NTT Basic Research Laboratories  
Atsugi-shi, 243-0198 Japan  
E-mail: oguri@nttbl.jp

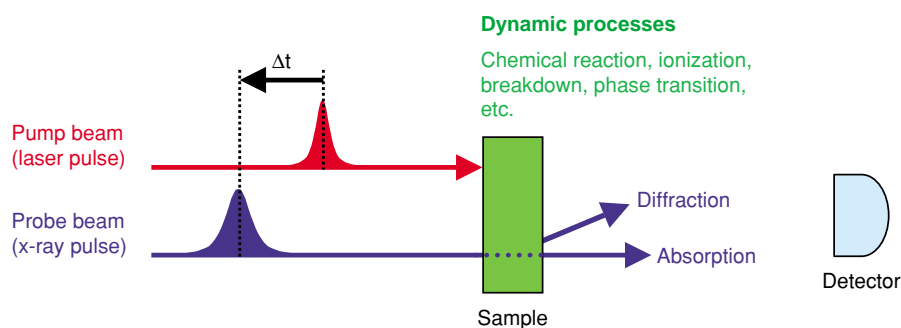


Fig. 1. Basic concept of time-resolved x-ray techniques.

which has long been a dream of scientists. From this point of view, the interdisciplinary research field between x-ray science and ultrafast science has emerged as “ultrafast x-ray science”.

The concept of the time-resolved x-ray techniques is very simple (Fig. 1). A laser pulse (pump pulse) excites the sample, and then an x-ray pulse (probe pulse) with a variable time delay  $\Delta t$  with respect to the laser pulse is either scattered or absorbed by the sample. We can obtain information about the sample by detecting the scattered or absorbed x-rays, which correspond to x-ray diffraction and x-ray absorption, respectively. By tuning the time delay, we can measure the time evolution of the excited states. In particular, the fine structure that appears near the x-ray absorption edge in the x-ray absorption spectrum, known as the x-ray absorption fine structure (XAFS), is sensitive to local order such as the atomic arrangement, chemical bonding, and electronic states of the absorbing atom. XAFS is classified into two types: x-ray absorption near-edge structure (XANES) and extended x-ray absorption fine structure (EXAFS). These provide information about the electronic states and bond length of the absorbing atom, respectively. In addition, XAFS can provide local structural information about various types of material, while x-ray diffraction mainly provides information about the long-range structure of crystalline materials. Therefore, time-resolved XAFS measurement with a temporal resolution of a picosecond or better is thought to be an important tool for capturing ultrafast chemical reactions. Studies using ultrafast time-resolved XAFS are still in their early stages, and considerable effort is being made to establish it as a standard technique [3].

This paper describes our recent research on time-resolved x-ray absorption spectroscopy in which we used ultrashort x-ray pulses emitted from femtosecond-laser-produced plasma. Section 2 introduces the

main laser-based ultrashort x-ray sources, in particular, the laser-produced-plasma x-ray source that we have been developing. Section 3 describes the enhancement of the x-ray conversion efficiency achieved by using nanostructured targets. Section 4 reports our recent results for time-resolved XAFS measurements of Si using a laser-produced-plasma x-ray source.

## 2. Laser-based ultrashort x-ray sources

The key technology in a time-resolved XAFS measurement system is the laser-based ultrashort x-ray source. Sources can be classified into two types according to the physical mechanism of x-ray production. One is laser high-order harmonics produced by the nonperturbative nonlinear response of gaseous atoms to a strong laser field with an intensity of about  $10^{13}$ – $10^{14}$  W/cm<sup>2</sup> [4]. Its spectrum exhibits well-resolved discrete odd-order harmonics ranging typically from 10 to 100 eV. The second is a laser-produced-plasma x-ray source that can cover the x-ray region, especially from a few tens of electron volts to over 100 keV [5]. This source utilizes the thermal x-ray emission from high-density high-temperature plasma created on a target surface by laser irradiation with an intensity of about  $10^{15}$ – $10^{18}$  W/cm<sup>2</sup>. In general, the characteristics of the emission spectrum depend strongly on the target material, i.e., strong line emissions are dominant in the spectrum for lighter elements (e.g., C, Al, and Si), while broadband emission with less pronounced line emission is dominant in the spectrum for heavier elements (e.g., Au, Ta, and W). When the laser intensity is about  $10^{16}$ – $10^{18}$  W/cm<sup>2</sup>, the plasma emits continuous and characteristic x-rays in the keV region, so it is often called a laser-driven electron x-ray source. This keV-x-ray emission is based on the bremsstrahlung and  $K_{\alpha}$  radiation of fast electrons accelerated by the steep

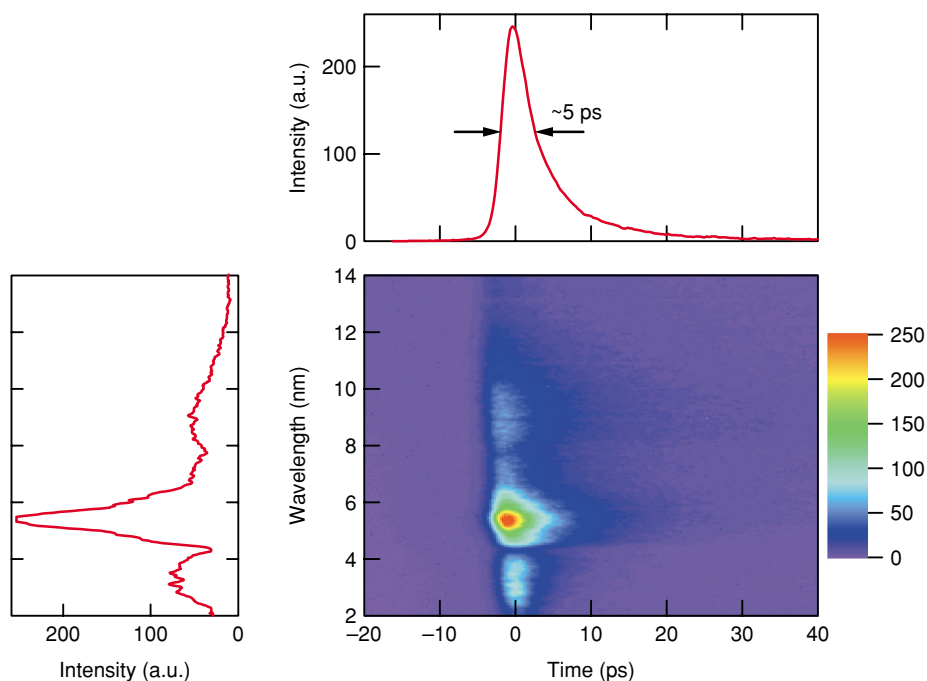


Fig. 2. Temporally and spectrally resolved soft x-ray emission from Ta target at a laser intensity of  $\sim 10^{16}$  W/cm<sup>2</sup>. The spectral profile at the maximum intensity and the temporal profiles at 5.5 nm are also plotted.

intensity gradient of the high-peak-power laser pulse.

In particular, we have been intensively studying the generation of x-rays from femtosecond-laser-produced-plasma because these x-rays possess an ultrashort pulse duration of the picosecond or sub-picosecond order as well as a high x-ray fluence. This makes them good x-ray sources for time-resolved x-ray techniques. The other important reason is that the smooth broadband spectrum of laser-produced-plasma x-rays generated from heavy elements is suitable for XAFS measurements. **Figure 2** shows a spectrally resolved x-ray streak image of a laser-produced-plasma x-ray pulse from a Ta target, its spectrum at the maximum intensity, and its pulse shape at 5.5 nm. Although the x-ray intensity in the longer wavelength region is relatively low due to the photon-energy dependence of the quantum yield of the CsI photocathode of the x-ray streak camera, the spectrum is smooth without any line emission. The pulse shape exhibits a steep rise and a slow decay caused by the thermal emission from high-temperature plasma. The pulse duration is about 5 ps, which determines the limit on the temporal resolution of our time-resolved XAFS system.

### 3. Nanostructured target to enhance x-ray intensity

When femtosecond-laser-produced-plasma x-rays are used as an ultrashort-pulse source for time-resolved XAFS, a sufficiently large x-ray fluence is essential to obtain a good-quality absorption spectrum. Methods for improving the conversion efficiency of laser-produced-plasma-x-ray generation can be categorized into two approaches. One is to introduce a weak prepulse before the main pulse to generate preformed plasma [7], [8]. In general, x-ray generation from a laser pulse does not have very high energy conversion efficiency because the energy of the laser pulse is mostly reflected by the surface of the target, especially in the case of metal targets. The low-density expanding preplasma generated by the prepulse can absorb the energy of the main strong laser pulse efficiently, so the conversion efficiency is higher. This method can control the x-ray fluence, x-ray pulse duration, and spectrum distribution by controlling the prepulse and main-pulse conditions, i.e., the pulse intensity ratio and separation time. However, this method inevitably leads to a broadening of the resultant x-ray pulse as a result of the low heat conductivity of the preplasma between the target and the main plasma [8]. The other approach involves using a

target with a structured surface having a low average density and a high local density [9], [10]. Here, we introduce two novel types of target with artificially designed nanostructured surfaces. Since the large surface area of the nanostructured targets increases the region of interaction with the laser pulse, the conversion efficiency increases as a result of the efficient absorption of the laser pulse energy. In contrast to the prepulse method, the pulse broadening effect is suppressed because the region with high local density retains high heat conductivity.

One type is an alumina nanohole-array target formed using the self-organization process of the anodic oxidation of an aluminum plate [11]. We obtained the x-ray emission spectrum from this target irradiated by a Ti:sapphire laser pulse with an intensity of  $1.5 \times 10^{16}$  W/cm<sup>2</sup> as shown in Fig. 3, which also shows the spectrum from an ordinary alumina plate target with a flat surface for comparison. Note that the intensity scale on the flat alumina plate is expanded by a factor of ten. The inset in Fig. 3 shows a top-view scanning electron microscope (SEM) image of the alumina nanohole-array target with a hole pitch of 100 nm, hole diameter of about 90 nm, and hole depth of about 40  $\mu$ m. This figure clearly shows that an approximately 30-fold enhancement of soft x-ray intensity was achieved in the wavelength region from 7 to 20 nm. The appearance of line emission from the Al<sup>5+</sup> and Al<sup>8+</sup> ions in the short-wavelength region implies that ionization to the higher charged state was promoted by the increase in elec-

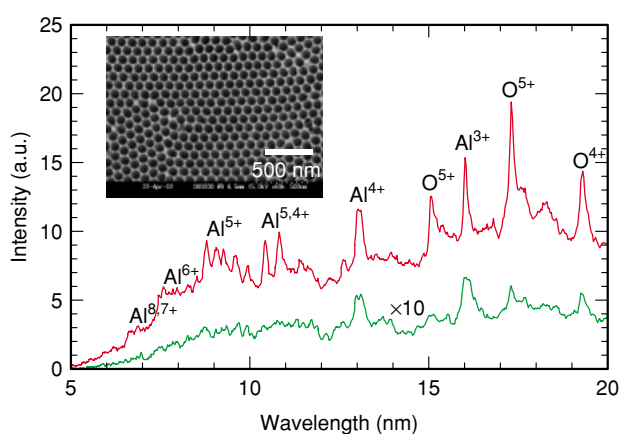


Fig. 3. Time-integrated soft x-ray spectrum from an alumina nanohole-array target (red). The spectrum from an ordinary flat alumina plate (green) is shown for comparison (note the scale is  $\times 10$ ). The inset shows a top-view SEM image of an anodic alumina nanohole-array target.

tron temperature caused by the efficient energy absorption of this target. In addition, we confirmed that there was a 20-fold x-ray intensity enhancement in the same wavelength region when we used a gold nanocylinder-array target, which was made by filling the nanoholes in the anodic alumina with gold by electrodeposition and removing the alumina part [12].

The other nanostructured target is a carbon nanotube (CNT), which is made by microwave plasma-enhanced chemical vapor deposition [14]. Carbon exhibits strong emission lines around 4 nm, which correspond to the “water window” region (2.3–4.4 nm). The x-ray pulse in this region is suitable for the x-ray microscopic imaging of biological specimens because the natural contrast between protein and water can be obtained due to the large absorption differences between carbon and oxygen. For this purpose, x-ray sources that have sufficient x-ray fluence have been required. The inset in Fig. 4 shows a side-view SEM image of a CNT target. Vertically aligned multiwalled nanotubes were formed with a spacing of about 150 nm on a silicon substrate. They are 30 nm in diameter and 12  $\mu$ m high. Figure 4 also shows the emission spectrum from an ordinary carbon plate and several types of CNT targets when the intensity of the incident laser pulse on the target was about  $3.7 \times 10^{16}$  W/cm<sup>2</sup>. Line emissions from the helium-like carbon ions, He $\alpha$  and He $\beta$ , and from the hydrogen-like carbon ions, Ly $\alpha$ , Ly $\beta$ , and Ly $\gamma$ , were observed in the water-window region. This figure also clearly shows

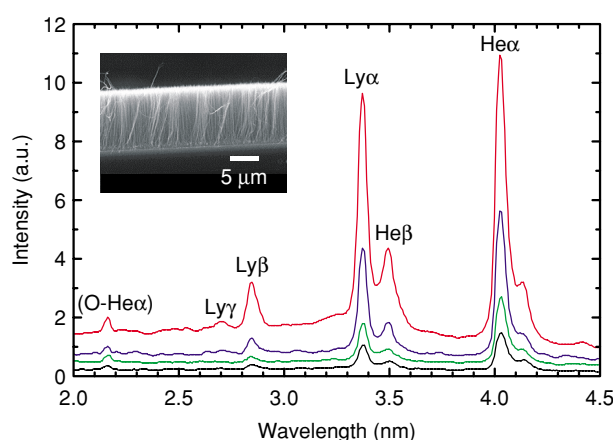


Fig. 4. Time-integrated soft x-ray spectra in the water-window region from vertically aligned multiwalled CNT (red), unaligned multiwalled CNT (blue), unaligned single-walled CNT (green), and an ordinary carbon plate targets (black). The inset shows a side-view SEM image of the vertically aligned multiwalled CNT target.

that an approximately 7-fold soft x-ray intensity enhancement was achieved with the aligned multi-walled CNT. The number of photons obtained in the water-window region was estimated to be  $2 \times 10^{12}$  photons/steradian per pulse. A general comparison of laser-produced-plasma x-ray sources with other conventional x-ray sources, such as rotating anode tubes, is difficult because the former are pulse sources while the latter are continuous wave (cw) sources. However, it is generally true that laser-produced-plasma x-ray sources produce x-rays with much higher peak power but lower average power than rotating anode tubes do. When we convert the number of photons obtained from the CNT targets into the peak spectral brightness, which represents the peak photon flux emitted per unit time (s), unit source size ( $\text{mm}^2$ ), unit solid angle ( $\text{mrad}^2$ ), and 0.1% bandwidth, it corresponds to approximately  $1 \times 10^{18}$  photons/s/ $\text{mm}^2/\text{mrad}^2/0.1\% \text{BW}$ . Since the peak spectral brightness of a rotating anode tube is typically  $\sim 10^8$  photons/s/ $\text{mm}^2/\text{mrad}^2/0.1\% \text{BW}$ , it is easy to see that the laser-produced-plasma x-ray source generates a huge number of photons in an extremely short time.

#### 4. Time-resolved XAFS measurement on laser-excited Si

Here, we describe an experimental demonstration of time-resolved XAFS measurement using a femtosecond laser-produced-plasma soft x-ray source. We used this system to measure the time evolution of the L-edge XAFS in Si foil under two different incident laser conditions: low intensity irradiation ( $\sim 10^{10}$

$\text{W}/\text{cm}^2$ ) [14] and high intensity irradiation ( $\sim 10^{12}$   $\text{W}/\text{cm}^2$ ) [15].

The experimental setup is schematically illustrated in **Fig. 5**. A laser pulse from a 100-fs Ti:sapphire laser with a central wavelength of 790 nm was fed to a beam splitter, where 80% of the energy was reflected. The reflected pulse was focused onto a Ta target at normal incidence to generate broadband soft x-ray pulses, as shown in Fig. 2. The emitted x-ray pulses were focused onto an amorphous Si sample with a thickness of about 100 nm by a condenser mirror. The transmitted x-ray pulses were again focused onto the entrance slit of a flat-field grazing incidence spectrograph and detected with a microchannel plate combined with a cooled charge-coupled device. The remaining laser pulses that passed through the beam splitter were fed into an optical variable delay line and softly focused onto the sample. This is our basic design for a time-resolved XAFS system.

An example of the absorption spectrum of Si foil is shown in **Fig. 6**. We can clearly see the  $L_{\text{II,III}}$  edge at 99 eV and the  $L_{\text{I}}$  edge at 150 eV, which correspond to the spectrum components representing transitions from  $2p$  to  $3s$  and from  $2s$  to  $3p$  in the conduction band, respectively. Therefore, the XANES of the Si  $L_{\text{II,III}}$  edge almost corresponds to the total density of states (DOS) in the unoccupied conduction band. In the energy region from 160 to 270 eV, the absorption spectrum decreases with a slight oscillation, which corresponds to L-edge EXAFS. From an analysis of the EXAFS, we can obtain information about the Si-Si bond length in the Si sample.

First, we observed dynamic changes in the XANES

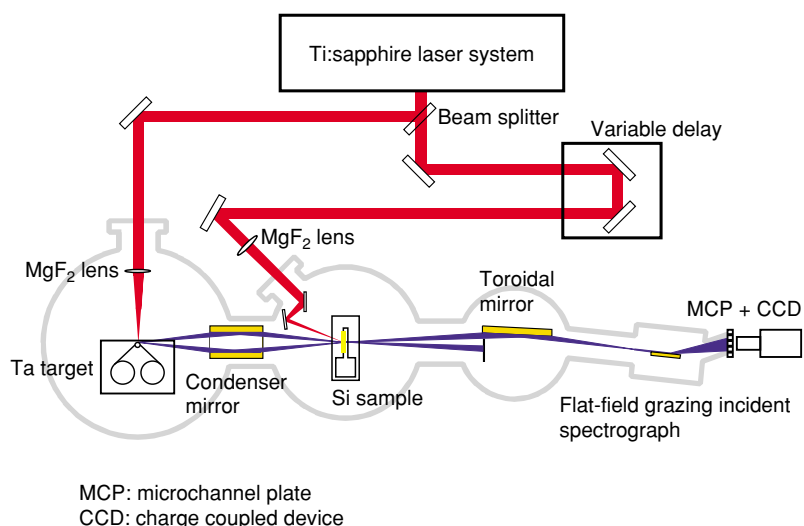


Fig. 5. Schematic illustration of the experimental setup for time-resolved XAFS.

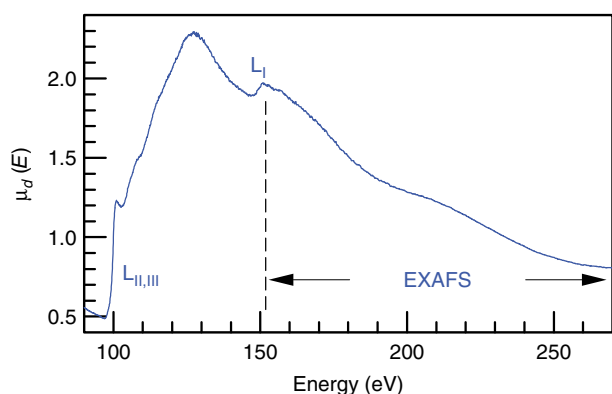


Fig. 6. Example of the absorption spectrum of amorphous Si foil with a thickness of 100 nm. Here,  $\mu_d(E)$  is an absorption coefficient defined by  $\mu_d(E) = \ln[I_0(E)/I(E)]$ , where  $E$ ,  $I_0(E)$ , and  $I(E)$  are the photon energy, the emission, and the transmission spectra, respectively.

of the  $L_{II,III}$  edge when the sample was irradiated by a laser pulse with an intensity of  $3 \times 10^{10} \text{ W/cm}^2$ , which is well below the damage threshold. Typical transmission spectra with and without laser irradiation are shown in **Fig. 7(a)**. Also shown is the differential transmittance between these two spectra. We observed a significant dip in the differential transmittance at 99.5 eV, which corresponds to the energy difference between the  $L_{II,III}$  level and the top of the valence band [16]. In **Fig. 7(b)**, the depth of the dip in the differential transmittance is plotted as a function of the time delay of the soft x-ray pulse with respect to the laser pulse. Zero delay represents the x-ray and the laser pulse peaks overlapping. This figure shows that the dip at 99.5 eV appeared only when the time delay was from  $-20$  ps to 40 ps. In this figure, the increase in the dip depth corresponds to the shape of the soft x-ray-pulse when the time delay was negative, i.e., when the soft x-ray pulse passed through the sample before the laser pulse arrived. This indicates that the change in transmission of the sample occurred immediately after the laser irradiation. On the other hand, the recovery time from the change in the transmission can be estimated to be about 16 ps from the decrease in the dip depth in the positive-delay region. The simplest model for explaining the laser induced absorption change shown in Fig. 7 involves the addition of a new absorption line. In semiconductors, transitions from the core level to the valence band are usually prohibited because the valence band is occupied. However, in photoexcited semiconductors, holes (i.e., vacancies) are created in the valence band. These vacancies allow the transi-

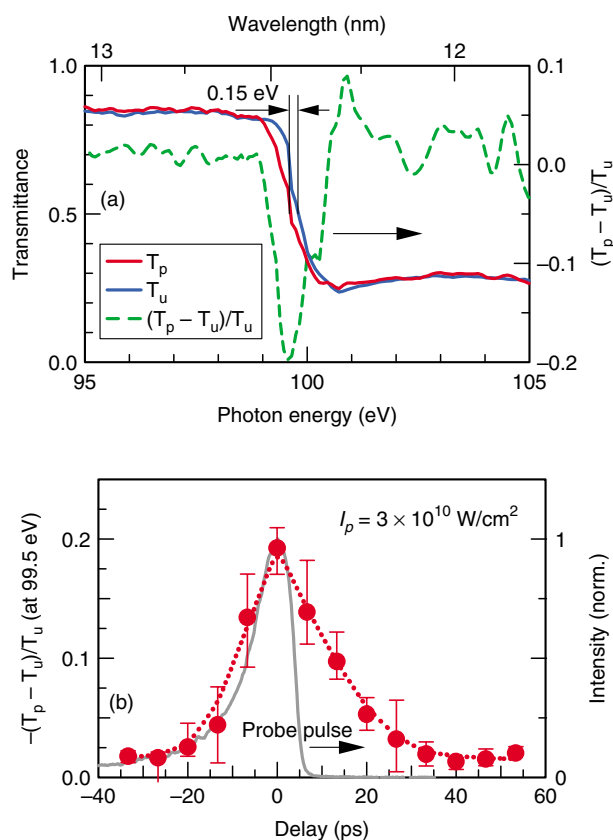


Fig. 7. (a) Transmission spectra of Si foil near the  $L_{II,III}$  edge. The red and blue curves represent transmission spectra with and without laser irradiation, respectively. The dashed green curve is the differential transmission spectrum between these two spectra. We defined the differential transmittance as  $(T_P - T_U)/T_U$ , where  $T_P$  and  $T_U$  represent the Si transmittance with and without the pump beam, respectively. (b) Differential transmittance at 99.5 eV as a function of the time delay when the intensity of the laser pulse was  $3 \times 10^{10} \text{ W/cm}^2$ . The pulse shape of the soft x-ray pulse (probe pulse) is also plotted in this figure (gray).

tion from the core level to the top of the valence band, so the soft x-ray absorption at 99.5 eV increases. The good agreement between the recovery time estimated from Fig. 7(b) and the recombination time of an electron-hole pair supports the validity of our physical model.

Second, we observed the time evolution of the L-edge EXAFS when laser pulses with an intensity of  $5 \times 10^{12} \text{ W/cm}^2$  excited the sample. In this case, since the excitation intensity was well above the damage threshold, the sample was ablated by each laser shot. Therefore, we scanned the sample to refresh the laser irradiation region for each laser shot. **Figure 8** shows

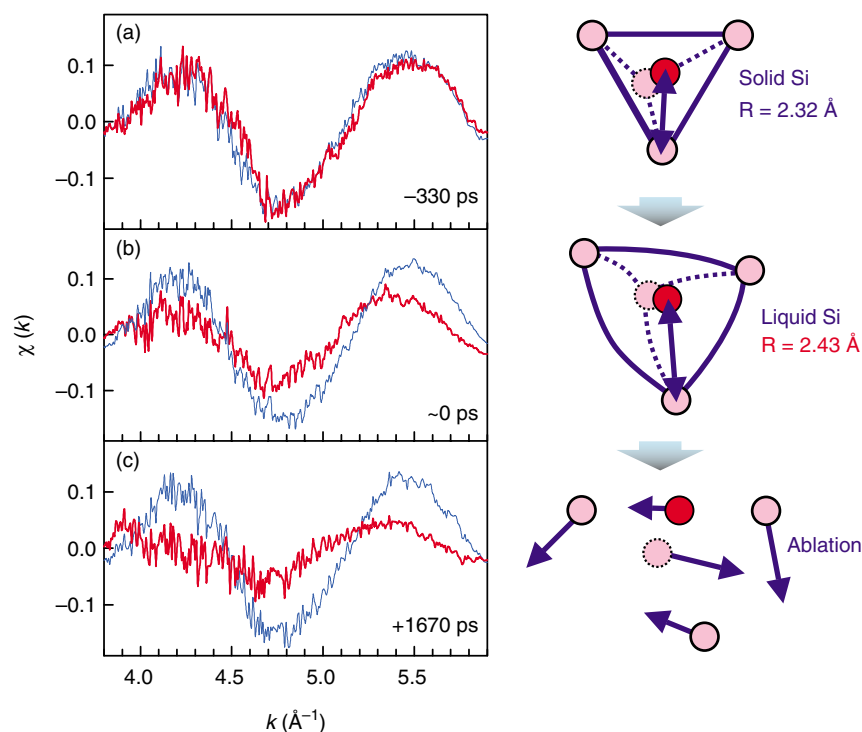


Fig. 8. Transient EXAFS spectra for various time delays (red line) when the intensity of the laser pulse was  $5 \times 10^{12}$  W/cm<sup>2</sup>. The EXAFS function  $\chi(k)$  is defined as  $\chi(k) = [\mu(k) - \mu_0(k)]/\mu_0(k)$ , where  $k$  is the wave number of photoelectrons and  $\mu(k)$  and  $\mu_0(k)$  represent the absorption coefficient of the sample and that of an isolated atom, respectively. Data for the unpumped condition is also shown for comparison (blue line).

the time evolution of the EXAFS spectra obtained from the absorption spectra in Fig. 6. When the x-ray pulse passed through the Si sample 330 ps before the arrival of the laser pulse, no large difference was observed between the EXAFS spectra of the pumped (red curve) and unpumped (blue curve) samples (**Fig. 8(a)**). We obtained a Si-Si atomic distance of 2.32 Å by Fourier transformation of the EXAFS spectra. The good agreement between the obtained bond distance and previously reported values (2.35 Å) [17] confirmed the validity of the measurement. Next, as shown in **Fig. 8(b)**, we can clearly see that the EXAFS oscillation amplitude decreased with a small peak shift toward a lower wave number when the x-ray pulse almost overlapped the laser pulse. The decrease in the oscillation amplitude is probably caused by a mixture of thermal damping and structural disordering. Since the small peak shift indicates that the oscillation period became shorter than that of the unpumped Si, this strongly suggests that the Si-Si atomic distance broadened slightly due to the laser excitation. By the Fourier transformation of this EXAFS spectrum, we obtained a Si-Si atomic distance of 2.43 Å, which agrees well with the reported

value of 2.45–2.50 Å for liquid Si at 1700–1800 K [18], thus the increase in Si-Si atomic distance can be explained by the ultrafast production of liquid Si. At a time delay of +1670 ps, the EXAFS became too weak for us to analyze its oscillation structure (**Fig. 8(c)**). The disappearance of the oscillation structure indicates further structural disordering of Si due to the onset of evaporation from the liquid phase to a gas-like phase. As discussed above, our study clearly shows that ultrafast structural changes during laser melting can be captured directly by using the time-resolved XAFS technique.

## 5. Summary

Time-resolved XAFS spectroscopy is expected to become a useful tool for detecting the processes that occur during the making and breaking of chemical bonds and during atomic rearrangements of various types of material, such as crystals, amorphous materials, and liquids. Laser-produced-plasma x-rays that have both a high x-ray fluence and a short pulse duration constitute a promising x-ray source for such spectroscopy. We conducted two experiments to

investigate this time-resolved XAFS technique based on a femtosecond-laser-produced-plasma x-ray source. One involved enhancing the x-ray fluence by fabricating an array of nanoholes on an Al surface or carbon nanotubes on a Si substrate. We achieved a large enhancement due to the enlargement of the interaction region between the laser pulse and the target surface. The other experiment involved measuring picosecond time-resolved XAFS for laser-excited Si foil. We found an increase in x-ray absorption near the  $L_{II,III}$ -edge structure as a result of the creation of vacancies in the valence band by laser irradiation with an intensity of  $\sim 10^{10}$  W/cm<sup>2</sup>. With a laser intensity of  $\sim 10^{12}$  W/cm<sup>2</sup>, we observed a slight shortening of the EXAFS oscillation period and a decrease in its oscillation amplitude. This can be explained by an increase in the Si-Si atomic distance and the structural disordering as a result of the production of liquid Si. This study clearly demonstrates the potential of the time-resolved XAFS technique for capturing ultrafast changes in the electronic state and atomic structure of materials.

### Acknowledgments

We thank Professor Hideki Masuda of Tokyo Metropolitan University and Dr. Otto Zhou of the University of North Carolina for providing us with the nanostructured targets, and Professor Naoshi Uesugi of Tohoku Institute of Technology for initiating this project and providing helpful suggestions and encouragement throughout this study. Financial support was provided by grant aid from the Ministry of Education, Culture, Sports, Science and Technology of Japan (Grant No. 16032219).

### References

- [1] A. H. Zewail, "Femtochemistry: Atomic-scale dynamics of the chemical bond," *J. Phys. Chem. A*, Vol. 104, pp. 5660-5694, 2000.
- [2] F. Rossi and T. Kuhn, "Theory of ultrafast phenomena in photoexcited semiconductors," *Rev. Mod. Phys.*, Vol. 74, pp. 895-950, 2002.
- [3] C. Bressler and M. Chergui, "Ultrafast x-ray absorption spectroscopy," *Chem. Rev.*, Vol. 104, pp. 1781-1812, 2004.
- [4] T. Brabec and F. Krausz, "Intense few-cycle laser fields: Frontiers of nonlinear optics," *Rev. Mod. Phys.*, Vol. 72, pp. 545-591, 2000.
- [5] M. M. Murnane, H. C. Kapteyn, M. D. Rosen, and R. W. Falcone, "Ultrafast x-ray pulses from laser-produced plasmas," *Science*, Vol. 251, pp. 531-536, 1991.
- [6] A. Rousse, P. Audebert, J. P. Geindre, F. Falliès, J. C. Gauthier, A. Mysyrowicz, G. Grillon, and A. Antonetti, "Efficient  $K\alpha$  x-ray source from femtosecond laser-produced plasmas," *Phys. Rev. E*, Vol. 50, pp. 2200-2207, 1994.
- [7] D. Kühlke, U. Herpers, and D. von der Linde, "Soft x-ray emission from subpicosecond laser-produced plasmas," *Appl. Phys. Lett.*, Vol. 50, pp. 1785-1787, 1989.
- [8] H. Nakano, T. Nishikawa, H. Ahn, and N. Uesugi, "Temporal evolution of soft x-ray pulse emitted from aluminum plasma produced by a pair of Ti:sapphire laser pulses," *Appl. Phys. Lett.*, Vol. 69, pp. 2992-2994, 1996.
- [9] M. M. Murnane, H. C. Kapteyn, S. P. Gordon, and R. W. Falcone, "Ultrashort X-ray pulses," *Appl. Phys. B*, Vol. 58, pp. 261-266, 1994.
- [10] T. Nishikawa, H. Nakano, H. Ahn, N. Uesugi, and T. Serikawa, "X-ray generation enhancement from a laser-produced plasma with a porous silicon target," *Appl. Phys. Lett.*, Vol. 70, pp. 1653-1655, 1997.
- [11] T. Nishikawa, H. Nakano, N. Uesugi, M. Nakao, K. Nishio, and H. Masuda, "Greatly enhanced soft x-ray generation from femtosecond-laser-produced plasma by using a nanohole-alumina target," *Appl. Phys. Lett.*, Vol. 75, pp. 4079-4081, 1999.
- [12] T. Nishikawa, H. Nakano, K. Oguri, N. Uesugi, M. Nakao, K. Nishio, and H. Masuda, "Nanocylinder-array structure greatly increases the soft X-ray intensity generated from femtosecond-laser-produced plasma," *Appl. Phys. B*, Vol. 73, pp. 185-188, 2001.
- [13] T. Nishikawa, K. Oguri, S. Suzuki, Y. Watanabe, O. Zhou, and H. Nakano, "Enhanced water-window x-ray pulse generation from femtosecond-laser-produced plasma with a carbon nanotube target," *Jpn. J. Appl. Phys.*, Vol. 42, pp. L990-L992, 2003.
- [14] H. Nakano, Y. Goto, P. Lu, T. Nishikawa, and N. Uesugi, "Time-resolved soft x-ray absorption spectroscopy of silicon using femtosecond laser-plasma x-rays," *Appl. Phys. Lett.*, Vol. 75, pp. 2350-2352, 1999.
- [15] K. Oguri, Y. Okano, T. Nishikawa, and H. Nakano, "Transient observation of extended x-ray absorption fine structure in laser melted Si by using femtosecond laser-produced-plasma soft x ray," *Appl. Phys. Lett.*, Vol. 87, 011503, 2005.
- [16] C. V. Shank, R. Yen, and C. Hirlimann, "Time-resolved reflectivity measurements of femtosecond-optical-pulse-induced phase transitions in silicon," *Phys. Rev. Lett.*, Vol. 50, pp. 454-457, 1983.
- [17] K. Laaziri, S. Kycia, S. Roorda, M. Chicoine, J. L. Robertson, J. Wang, and S. C. Moss, "High-energy x-ray diffraction study of pure amorphous silicon," *Phys. Rev. B*, Vol. 60, pp. 13520-13533, 1999.
- [18] Y. Waseda, K. Shinoda, K. Sugiyama, S. Takeda, K. Terashima, and J. M. Toguri, "High temperature x-ray diffraction study of melt structure of silicon," *Jpn. J. Appl. Phys.*, Vol. 34, pp. 4124-4128, 1995.



**Katsuya Oguri**

Quantum Optical Physics Research Group, Optical Science Laboratory, NTT Basic Research Laboratories.

He received the B.S. and M.S. degrees from the University of Tokyo, Tokyo in 1996 and 1998, respectively. He joined NTT Basic Research Laboratories in 1998. Since then, he has been engaged in the study of high-power femtosecond-laser-based x-ray sources and their application. His current interest is ultrafast x-ray spectroscopy with laser-produced-plasma x-rays and high-order harmonics. He is a member of the Japan Society of Applied Physics (JSAP) and the Optical Society of America (OSA).

---



**Tadashi Nishikawa**

Senior Research Scientist, Quantum Optical Physics Research Group, NTT Basic Research Laboratories.

He received the B.S., M.S., and Ph.D. degrees from Tokyo Institute of Technology, Tokyo in 1986, 1988, and 1998, respectively. He joined NTT Basic Research Laboratories, Tokyo in 1988. In 2004, he received the 26th Japan Society of Applied Physics JJAP (Japanese Journal of Applied Physics) Best Original Paper Award. He is a member of JSAP.

---



**Yasuaki Okano**

Research Associate, Quantum Optical Physics Research Group, Optical Science Laboratory, NTT Basic Research Laboratories.

He received the B.E. degree in engineering from Saitama University, Saitama and the M.S. and Ph.D. degrees in science and engineering from Tokyo Institute of Technology, Kanagawa in 1999, 2001, and 2004, respectively. He joined NTT Basic Research Laboratories in 2004. He is a member of JSAP and the Japan Intense Light Field Science Society (JILS).

---



**Hidetoshi Nakano**

Senior Research Scientist, Group Leader, Quantum Optical Physics Research Group, Optical Science Laboratory, NTT Basic Research Laboratories.

He received the B.S. and M.S. degrees in electronic engineering, and the Ph.D. degree in electrical engineering from the University of Tokyo, Tokyo in 1982, 1984, and 1987, respectively. He joined NTT Basic Research Laboratories in 1987. Since then, he has been engaged in ultrafast optical physics research including applications of intense laser-field and ultrashort wavelength sources. He is a member of JSAP, the Institute of Electronics, Information and Communication Engineers of Japan, the Physical Society of Japan, the Laser Society of Japan, JILS, IEEE, OSA, and the International Society for Optical Engineering.

---